



**A STUDY OF SPHERICAL, PSEUDOSPHERICAL
AND CYLINDRICAL MODERATORS FOR A NEUTRON
DOSE EQUIVALENT RATE METER**

M. Awschalom, T. Borak & H. Howe

July 12, 1971

The properties of neutron detectors based on spherical polyethylene moderators with $\text{Li}^6\text{I}(\text{Eu})$ crystals at their center were described by Bonner¹⁾. He also indicated the usefulness of the system using the 12 inch diameter moderator as a neutron dosimeter. Hankins²⁾ showed that the 10 inch diameter moderator was also very good for neutron dosimetry. Other authors³⁻⁷⁾ have discussed the use of sets of these detectors as 4π neutron spectrometers as well as for routine radiation safety⁸⁻¹¹⁾.

Bonner spheres were selected for neutron moderators in the early days of NAL. Here, some of the problems associated with their use are discussed. The particular topics examined are:

1. the costs of machining spherical moderators,
2. neutron detection efficiency as a function of polar angle,
3. dose equivalent rate per count rate,
4. properties of a silver wrapped GM tube as a thermal neutron detector, and
5. variation in neutron detection efficiency due to different moderator densities.

We will present some measurements which have bearing on problems 1, 2, 3, & 4. Also, we will present our views on problem 5.

Cost of Machining Moderators. If, to a first approximation and at constant density, the energy response of the neutron detector depends on the volume of the moderator, then slight topological variations of the spherical shape should produce detectors of essentially similar responses. Hence, several equal volume simple shapes with cylindrical symmetry were made. In order of decreasing machining cost (see Appendix), they were,

- a) a sphere,
- b) a pseudosphere (a pseudosphere is generated when a regular octagon rotates about one median),
- c) a cylinder.

The cross sections for these detectors are shown in Figure 1, in their respective proportions. As it may be seen, the pseudosphere is just slightly different from the sphere.

The density of the linear polyethylene was between 0.924 and 0.927 g/cm³.

Figure 1 also shows the definition of the polar axis.

Variation of dosimeter sensitivity as a function of polar angle. Two different thermal neutron detectors were used,

- a) a 4mm high x 4mm diameter $\text{Li}^6\text{I}(\text{Eu})$ crystal, coupled via a half inch diameter plexiglass light pipe to a photomultiplier,
- b) an Amperex #18550, thin wall (0.030 g/cm^2) GM counter wrapped with a 0.010 inch thick silver foil (0.267 g/cm^2) or with an equal thickness in g/cm^2 of tin (0.014 inch).

Appropriate precautions were taken to center the detectors within the moderators. Standard nuclear electronics were used for counting and timing.

In the case of the silver activation, a waiting period of 15 minutes (or 6.3 half-lives of ^{108}Ag) was allowed before any data was taken. This provides a counting rate within 0.2% of the final counting rate, since the relative detectable activities from the ^{108}Ag and ^{110}Ag are 1.0 and 5.3, respectively (see Figure 2). Angular variations in counting rate were always less than a factor of two.

Neutron Source. The only neutron source conveniently available was a $^{238}\text{PuBe}$. It was calibrated by the NBS, which gave a total source strength (using the Mn SO_4 bath technique) of $1.89 \times 10^7 \text{ n/sec}$.

The flux-to-dose conversion factor for this source was assumed to be equal to that for a $^{239}\text{PuBe}_{13}$. A value of $3.52 \times 10^{-8} \text{ rem}/(\text{n}/\text{cm}^2)$ was taken for this source from the work of Nachtigall¹²⁾. Nachtigall also quotes conversion factors for kerma ($3.73 \times 10^{-9} \text{ rad}/(\text{n}/\text{cm}^2)$) and maximum dose in tissue ($4.70 \times 10^{-9} \text{ rad}/(\text{n}/\text{cm}^2)$).

Lawrence¹³⁾ reports 92% of the dose from a PuBe source to be due to neutrons and 8% due to 4.44 MeV gamma-rays.

Thus, the source was assumed to produce the radiation fields listed in Table I.

Table I
NEUTRON SOURCE PARAMETERS (PuBe-54)

flux (@ 1m)	$= 1.89 \times 10^7 / (4\pi \times 10^4)$	
	$= 1.50 \times 10^2 \text{ n}/\text{cm}^2 \text{ sec}$	
maximum tissue dose		
rate (@ 1m)	$= 4.70 \times 10^{-9} \times 1.50 \times 10^2 = 7.05 \times 10^{-7} \text{ rad}/\text{sec}$	
	$= 7.05 \times 10^{-7} \times 3.6 \times 10^3 = 2.54 \text{ mrad}/\text{hr}$	
kerma rate* (@ 1m)	$= 3.73 \times 10^{-9} \times 1.50 \times 10^2 = 5.60 \times 10^{-7} \text{ "rad"}/\text{sec}$	
	$= 5.60 \times 10^{-7} \times 3.6 \times 10^3 = 2.01 \text{ "mrad"}/\text{hr}$	
dose equivalent		
rate (@ 1m)	$= 3.52 \times 10^{-8} \times 1.50 \times 10^2 = 5.28 \times 10^{-6} \text{ rem}/\text{sec}$	
	$= 5.28 \times 10^{-6} \times 3.6 \times 10^3 = 19 \text{ mrem}/\text{hr}$	
gamma dose rate	$= 2.54 \times 8/92$	$= .022 \text{ mrem}/\text{hr}$

* actually the kerma rate should be expressed in ergs/gm.

Experimental Arrangement. To simplify data taking, a thin, counterbalanced aluminum arm was pivoted above the detector, giving a constant 73.8 cm distance between the centers of the neutron source and the detector (see Figure 3). In this figure, the source holder is seen screwed to a sphere which is supported by a cardboard tube which rests on top of other low mass supports.

Figure 4 is a photograph of the photomultiplier assembly without the holder and iron flange.

Figure 5 is a photograph of the Ag covered GM tube assembly.

Results. Figure 6 presents the relative polar angle response of the three moderators using a 4mm ϕ x 4mm high $^6\text{LiI(Eu)}$ crystal.

These results were taken with assemblies mounted without holder in order to minimize the interference from the iron holder and flange.

Wall scattering effects were studied by rotating the entire assembly, but keeping the source at 0° . At all positions the count rate was independent of the walls within statistical errors.

Figure 7 shows the responses of the sphere and pseudosphere with their holders and mounting flanges in place. The response of the sphere without holder or flange is added for comparison.

As it may be easily seen and as it may have been expected, the flange and holder affect the detection efficiency of only a small polar region.

Figure 8 shows the relative response of a pseudosphere with holder and mounting hardware and having either a $^6\text{LiI}(\text{Eu})$ crystal or an Ag wrapped GM tube. For all practical purposes, there is no difference in the polar responses of these two systems. Fifteen minutes delay time was allowed before taking a reading when using the Ag wrapped GM tube to permit stabilization of the counting rate.

In all the measurements, some right-left asymmetry may be seen. This is believed to be some remanent error in the axial alignment of the $\text{LiI}(\text{Eu})$ crystal.

The detection efficiency for PuBe neutrons is thus seen to be essentially indistinguishable between the sphere and the pseudosphere. On the other hand, the right cylinder shows variations about the "mean" of $\pm 10\%$.

Dose Equivalent Measurements. The dose equivalent per neutron per cm^2 is taken from Table I for PuBe. From measurements taken using a simple 4mm diameter, 4mm high $^6\text{LiI}(\text{Eu})$ crystal, we get the following flux-to-dose conversion factors.

Table II

⁶LiI(Eu) PuBe dose equivalent per count for
a crystal 4mm ϕ x 4mm high, at 0° and 90°

<u>Moderator</u>	$\frac{\text{rem}}{\text{count}}$ 0°	$\frac{\text{rem}}{\text{count}}$ 90°	$\frac{(\text{mrem/hr})}{(\text{count/sec})}$ 90°
Sphere	2.18×10^{-7}	2.18×10^{-7}	.785
Pseudosphere	2.21×10^{-7}	2.17×10^{-7}	.781
Cylinder	2.15×10^{-7}	1.97×10^{-7}	.709

For the type of neutron spectrum expected outside a thick soil shield, the rem per count may be calculated using the Bonner sphere response as given in reference 4, the PuBe as given by Brock and Anderson and also Stewart¹⁵⁾ and the neutron spectrum as given by K. O'Brien¹⁶⁾. Then, the ratio

$$\frac{(\text{rem/count})_{\text{accel}}}{(\text{rem/count})_{\text{PuBe}}} = \frac{\int_{0 \text{ acc}}^{200 \text{ GeV}} \phi(E') DE(E') dE' / \int_{0 \text{ acc}}^{200 \text{ GeV}} \phi(E') dE'}{\int_{0 \text{ PuBe}}^{10.5 \text{ MeV}} \phi(E') DE(E') dE' / \int_{0 \text{ PuBe}}^{10.5 \text{ MeV}} \phi(E') dE'}$$

may be evaluated to the best of our present knowledge.

The numerical calculations give,

$$(\text{rem/count})_{\text{accel}} = 5.51 \times 10^{-7}$$

$$(\text{rem/count})_{\text{PuBe}} = 2.17 \times 10^{-7}$$

Hence, $(\text{rem/count})_{\text{accel}} = 2.54 (\text{rem/count})_{\text{PuBe}}$ a useful ratio to use around NAL.

-8-

The Silver Wrapped Neutron Detector. The use of the ${}^6\text{LiI}(\text{Eu})$ crystal plus photomultiplier is very good in regions where counting rate losses are unimportant because of large duty cycle or low dose equivalent rates. In such circumstances, the ${}^6\text{LiI}(\text{Eu})$ crystal 4mm diameter x 4mm high, offers very good discrimination against gamma rays.

However, the Ag wrapped GM tube has advantages when low cost electronics are imperative and a small duty cycle is coupled with a sudden unexpected burst of neutrons. This technique was described in 1962 by A. R. Smith, but it may be older than that. The advantage of the Ag foil is that it provides a low cost neutron integrator with time constants of 24.4 sec (${}^{109}\text{Ag}(n,\gamma){}^{110}\text{Ag}$) and 2.4 minutes (${}^{107}\text{Ag}(n,\gamma){}^{108}\text{Ag}$).

The drawback of this technique is the sensitivity of the Ag-GM system to gamma rays.

Silver Thickness. Figure 9 shows the counting rate from the beta decay of ${}^{108}\text{Ag}$ and ${}^{110}\text{Ag}$, at constant geometry and flux versus Ag thickness as well as a similar curve for Rh. A thickness of 0.010 inch of Ag was adopted for the detectors. Advantages of Rh over Ag are the single, although longer, half-life of ${}^{104}\text{Rh}$ (42 sec) and its slightly greater sensitivity. However, the price of Rh is a serious disadvantage.

Naturally, a Ag wrapped GM tube is gamma-ray sensitive. However, this is not a problem when operating near a very short duty cycle accelerator since the pulses from the tube may be gated off during acceleration. However, when using a PuBe source for calibration, the gammas from the de-excitation of $^{12}\text{C}^*$, contribute significantly.

In order to remove the effects of the gamma-flux in the determination of the neutron dose, the gamma induced counting rate in the Ag wrapped tube was estimated using a Sn-wrap in place of the Ag around the same GM tube. The Sn-wrap (0.014 inch thick) had the equivalent thickness in g/cm^2 as the Ag wrap.

Two counting rate ratios were obtained, using the PuBe source mentioned in Table I, and the pseudosphere,

$$\frac{\text{Ag wrapped GM} - \text{bare GM}}{\text{Ag wrapped GM}} = 0.62 \pm 0.01$$

$$\frac{\text{Ag wrapped GM-Sn wrapped GM}}{\text{Ag wrapped GM}} = 0.66 \pm 0.01$$

Thus 2/3 of the counts from the PuBe source in a 0.010 inch thick Ag wrapped thin walled ($30\text{mg}/\text{cm}^2$) GM tube in a 10 inch pseudospherical moderator are due to neutron capture and subsequent beta counting. The conversion factor for a gamma-less PuBe like neutron spectrum for a 10 inch moderator and an Amperex #18550 GM tube wrapped in 10 mils of silver is

$$\text{Dose Equivalent Rate} = 1.31 (\text{mrem/hr})/(\text{count/sec}).$$

In one of the dose equivalent rate meters developed at NAL¹⁸⁾, two GM tubes are used. One is wrapped in 0.010 inch of Ag and the other one in 0.014 inch of Sn. Then, the outputs from these tubes are shaped and properly subtracted from each other. For adjustment of null output in a gamma-ray field, a Co-60 source has been used.

Sudden Fluxes (Impulse Approximation). One interesting capability of the Ag foil is its ability to integrate the neutron dose due to a very short burst of neutrons as in the case of an accident. Hence, in principle, it is always possible to calculate a neutron dose if a record of the Ag decay is available and the relative number of ^{108}Ag and ^{110}Ag nuclei is known.

For this purpose, a measurement of the ^{108}Ag and ^{110}Ag contributions to the counting GM, using 0.010 inch of Ag in a 10 inch moderator and a PuBe neutron source was carried out. A PuBe source was mounted on top of the pseudosphere for 30 minutes.

The output of the GM electronics was connected to the multichannel scale (MCS) input of a 4096 channel analyzer. The MCS was started and the source was very quickly removed.

-11-

From those results a least square fit to the data was made in which the half-lives of the $^{108,110}\text{Ag}$ were assumed known. The following expression was derived,

$$\text{CR}(t) = K[5.33 \exp(-0.693t/24.4 \text{ sec}) + 1.00 \exp(-0.693t/144 \text{ sec})]$$

where t is measured in seconds from the end of the irradiation and $\text{CR}(t)$ is the count rate in counts/sec (see Figure 2). K may have different meanings.

During a steady state condition when equilibrium has been reached by both silver isotopes, the counting rate is,

$$\text{CR} = K \dot{\text{DE}}$$

where,

K is the steady state dose rate-to-count rate conversion factor. From the measurements taken above,

$$\text{CR}(\text{c/sec}) = 0.763 (\text{c/sec}) / (\text{mrem/hr}) \times \dot{\text{DE}} (\text{mrem/hr})$$

OR

$$\text{CR}(\text{c/sec}) = 2.75 \times 10^6 (\text{c/sec}) / (\text{rem/sec}) \times \dot{\text{DE}} (\text{rem/sec}).$$

For the case when there is a large burst of neutrons for a very short time interval ($t_i \ll 24.4 \text{ sec}$) the counting rate can be represented by

$$\text{CR}(t_i, t) = k \dot{\text{DE}} \left\{ 5.33 [1 - \exp(-\lambda_1 t_i)] \exp(-\lambda_1 t) + 1.00 [1 - \exp(-\lambda_2 t_i)] \exp(-\lambda_2 t) \right\}$$

where,

$$\lambda_1 = \ln(2)/24.4 \text{ sec}$$

$$\lambda_2 = \ln(2)/144 \text{ sec}$$

-12-

t_i = irradiation time (i.e., duration of burst)

t = time measured from end of burst.

If $t_i \ll 24.4$ sec

$$CR(t_i, t) = 2.75 \times 10^6 (c/sec) / (rem/sec) \cdot DE(rem/sec) * \\ * [5.33\lambda_1 t_i \exp(-\lambda_1 t) + 1.00\lambda_2 t_i \exp(-\lambda_2 t)]$$

since $DE = DE \cdot t_i$

$$CR(t_i, t) = 2.75 \times 10^6 DE [5.33\lambda_1 \exp(-\lambda_1 t) + 1.00\lambda_2 \exp(-\lambda_2 t)]$$

The NAL Datalogger has the capability of recording the total counts over a given time interval, thus,

$$\text{Counts}(t, \Delta t) = \int_t^{t+\Delta t} CR(t_i, t) dt \\ = 2.75 \times 10^6 DE(rem) [5.33 \exp(-\lambda_1 t) (1 - \exp(-\lambda_1 \Delta t)) + \\ + 1.00 \exp(-\lambda_2 t) (1 - \exp(-\lambda_2 \Delta t))]]$$

Solving for DE

$$DE(rem) = \frac{3.64 \times 10^{-7} \text{ counts}(t, \Delta t)}{5.33 \exp(-\lambda_1 t) [1 - \exp(-\lambda_1 \Delta t)] + 1.00 \exp(-\lambda_2 t) [1 - \exp(-\lambda_2 \Delta t)]}$$

Assuming a typical case where the operator in charge records the total number of counts over a (5) minute interval, (5) minutes after the spill

$$DE(rem) = \frac{3.64 \times 10^{-7} \text{ counts}(300, 300)}{5.33 \times 1.99 \times 10^{-4} + .236 (1 - .236)} = \frac{3.64 \times 10^{-7} \text{ counts}(300, 300)}{(1.06 \times 10^{-3}) + (1.80 \times 10^{-1})}$$

Thus, under normal circumstances, the only contribution will be from the ^{108}Ag ($T_{1/2} = 144$ sec).

-13-

Variation of Neutron Detector Efficiency due to Different Moderator Densities. In this work we have assumed that the important parameter to determine the neutron detection efficiency is the total mass of the nearly spherical detector. We have based this on some early results of K. O'Brien¹⁶⁾.

Should the density vary from that used by Bonner¹⁾, we would expect that the important parameter will be $R\rho$, namely, that the typical dimension of the moderator, measured in mean-free paths will remain constant. Hopefully, this conjecture will soon be tested by some calculations to be done by R. Sanna¹⁹⁾.

APPENDIX

Estimated Cost of Materials and Machining of Moderators as Submitted by Cadillac Plastics,* Inc. Quotes are for quantities of twenty of each type.

Type	Unit Cost	Savings Per Unit
Sphere	\$312	--
Pseudosphere	\$264	\$48
Cylinder	\$232	\$80

*1245 West Fulton
Chicago, Illinois 60607

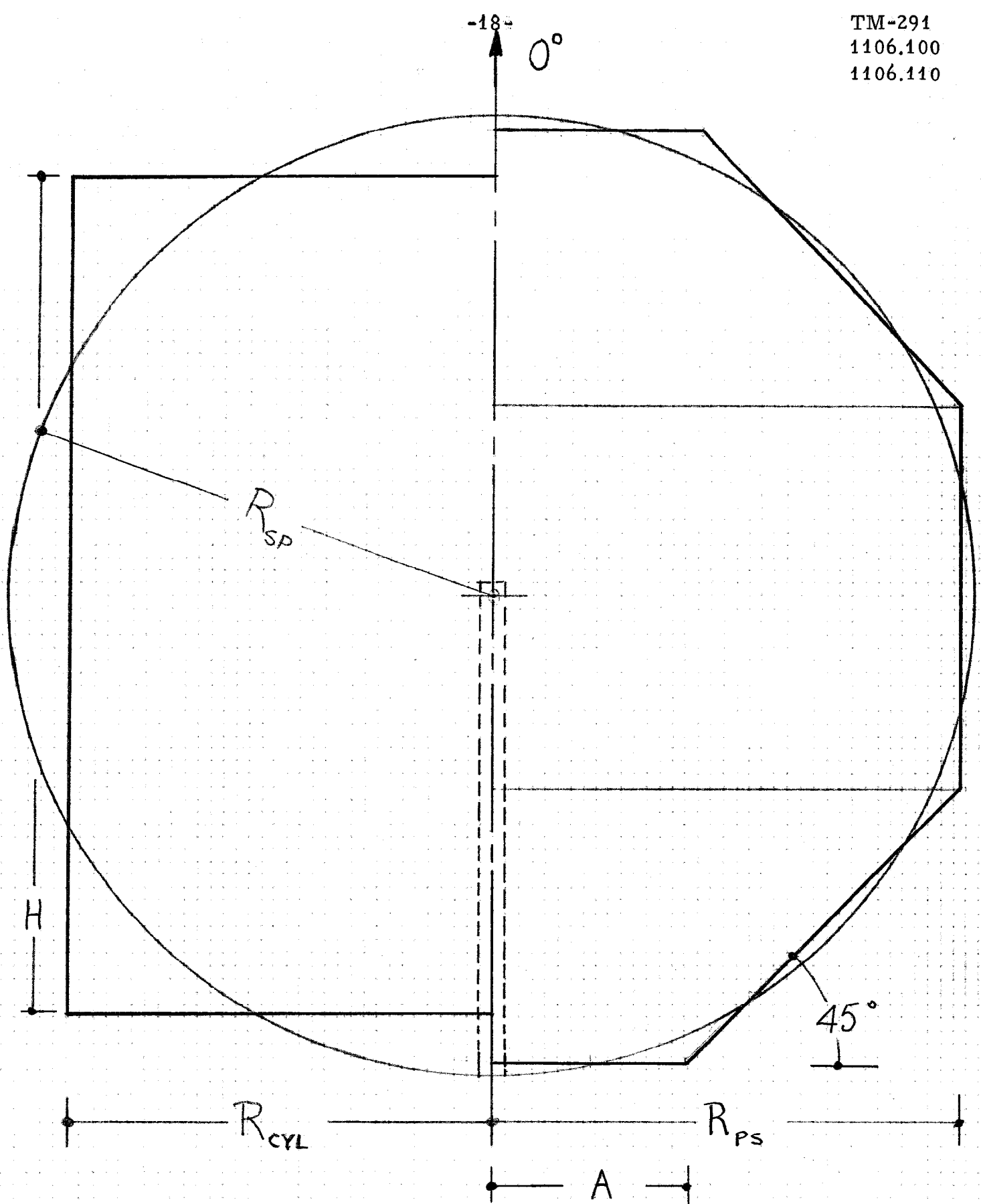
REFERENCES

1. R. L. Bramblett, et al., "A New Type of Neutron Spectrometer", Nucl. Instr. Meth. 9, 1 (1960).
2. a) D. E. Hankins, "A Method of Determining the Intermediate Energy Neutron Dose", IDO-16655 (March 10, 1961).
b) "A Neutron Monitoring Instrument . . .", LA-2717 (August 20, 1962).
3. M. Awschalom, "The Use of the Multisphere Neutron Detector . . .", Proc. IAEA Syrup Neutr. Monit. for Rad. Prot. Vienna, Aug. 29-Sept. 2, 1966.
4. A. S. Lazanoff & J. E. McLaughlin, "Feasibility Study of Using LiF Detectors . . .", HASL-206 (March, 1969).
5. M. Weinstein, et al., "Neutron Dose Equivalent . . .", HASL-223 (March, 1970).
6. M. Weinstein, et al., "Procedures for Estimating the Errors in Neutron Spectra . . .", HASL-TM-69-4.
7. G. L. Watkins & G. Holeman, "The Evaluation of an Iterative Technique . . .", Health Physics 15, 535 (1968).
8. D. E. Hankins, "Monitoring Intermediate Energy Neutrons", Health Physics 9, 31 (1963).
"The Multisphere . . . Technique", LA-3700 (June 7, 1968).
"A Modified-Sphere . . .", LA-3595 (Jan. 17, 1967).
9. D. E. Hankins & R. A. Pederson, "A Comparison of the Neutron Dose Rates . . .", LAMS-2977 (March 13, 1964).
10. D. Nachtigall & F. Rohloff, "Sphere Techniques . . .", SLAC-TR-23 (Sept. 1965).
11. J. W. Leake, "An Improved Spherical . . .", Nucl. Instr. Meth. 63, 329 (1968).

12. D. Nachtigall, "Average and Effective Energies, Fluence Dose Conversion Factors . . .", Health Physics 13, 213 (1967).
13. D. C. Lawrence, "Mixed Radiation Dosimetry . . .", Health Physics 7, 179 (1962).
14. M. Awschalom, et al., "Neutron Dosimetry . . .", TM-266 (Aug. 26, 1970).
15. a) H. W. Broek & C. E. Anderson, Rev. Sci. Instr. 31, 1063 (1960).
b) L. Stewart, Phys. Rev. 98, 740 (1955).
16. K. O'Brien, private communication.
17. A. R. Smith, UCRL-10163 (April, 1962).
18. M. Awschalom, et al., "Radiation Monitoring at NAL . . .", Int'l Cong. Prot. Against Acc. & Space Rad., CERN (April 26-30, 1971).
19. R. Sanna and K. O'Brien, private communication.

FIGURES

1. Cross-section of the three moderators used.
Sphere of radius = R
Pseudosphere,
Cylinder, $R_{\text{cyl}} = (2/3)^{1/3} R$
 $H_{\text{cyl}} = 2 R_{\text{cyl}}$
2. Decay of the count rate in a thin walled GM tube wrapped in Ag, after long irradiation by PuBe thermalized in a 10 inch pseudosphere.
3. Photograph of the experimental arrangement.
4. Photograph of the light pipe inserted in a pseudosphere, the photomultiplier and electronic hardware.
5. Photograph of the Ag wrapped GM tube assembly.
6. Polar response of dose-rate-meter as a function of polar angle. No flange or mounting hardware.
7. Polar response of sphere without flange or mounting hardware, and of sphere and pseudosphere with flange and mounting hardware.
8. Polar responses of pseudosphere with either a $^6\text{Li(Eu)}$ crystal or a silver wrapped GM tube.
9. Relative counting rates for a thin wall GM tube versus various thicknesses of either silver or rhodium.



CYLINDER

$$R_{CYL} = 0.8736 R_{SP}$$

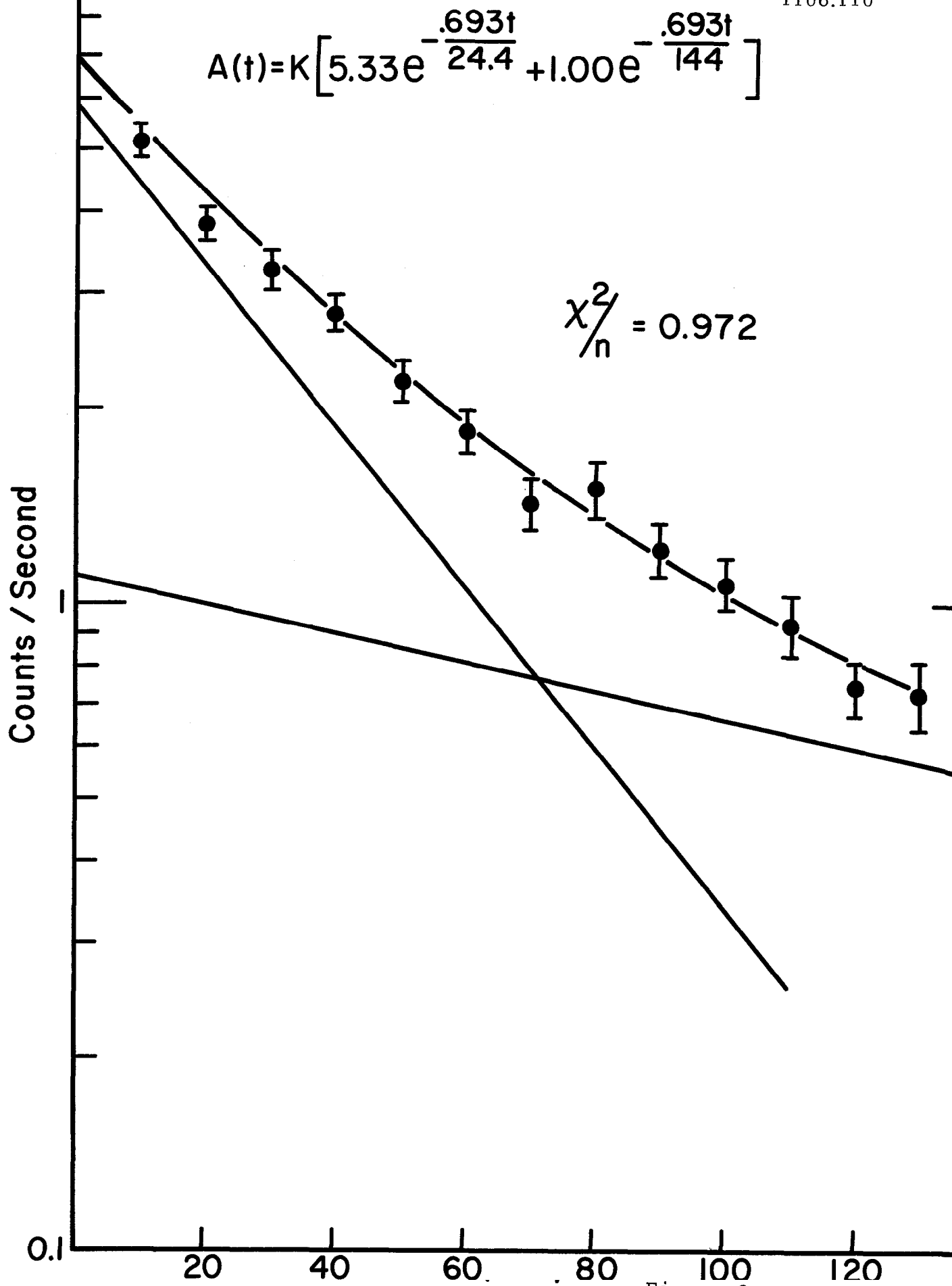
$$H = 2 R_{CYL}$$

PSEUDOSPHERE

$$R_{PS} = .9729 R_{SP}$$

$$A = .4030 R_{SP}$$

$$D = .5711 D$$



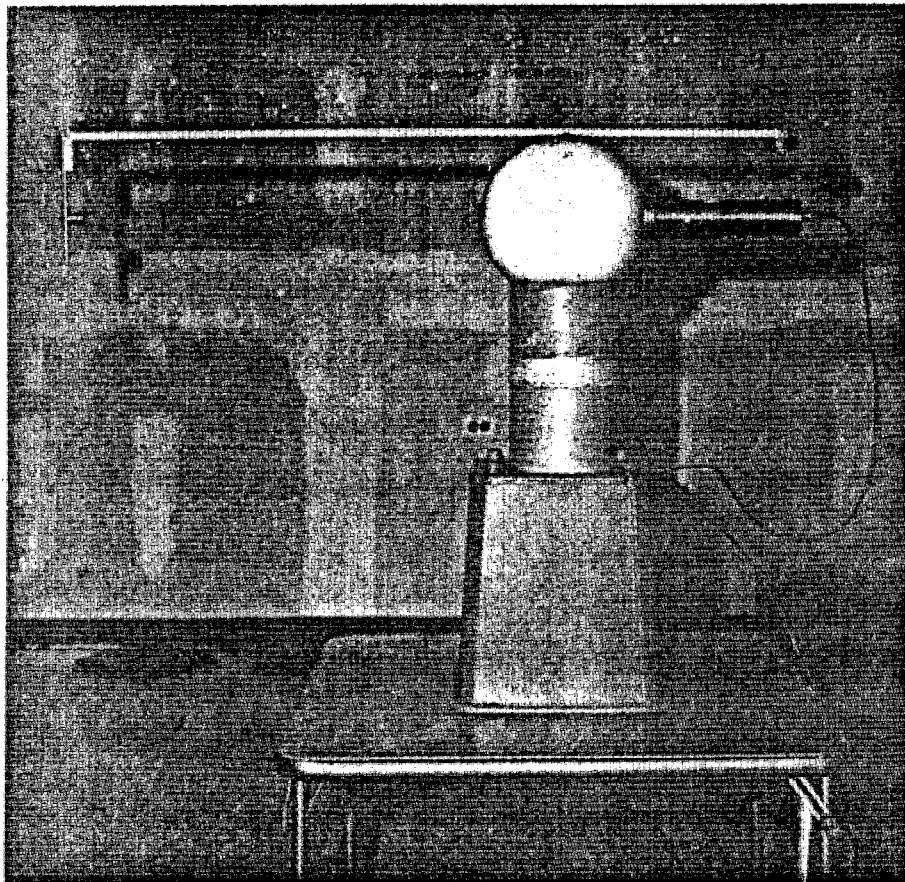


Figure 3

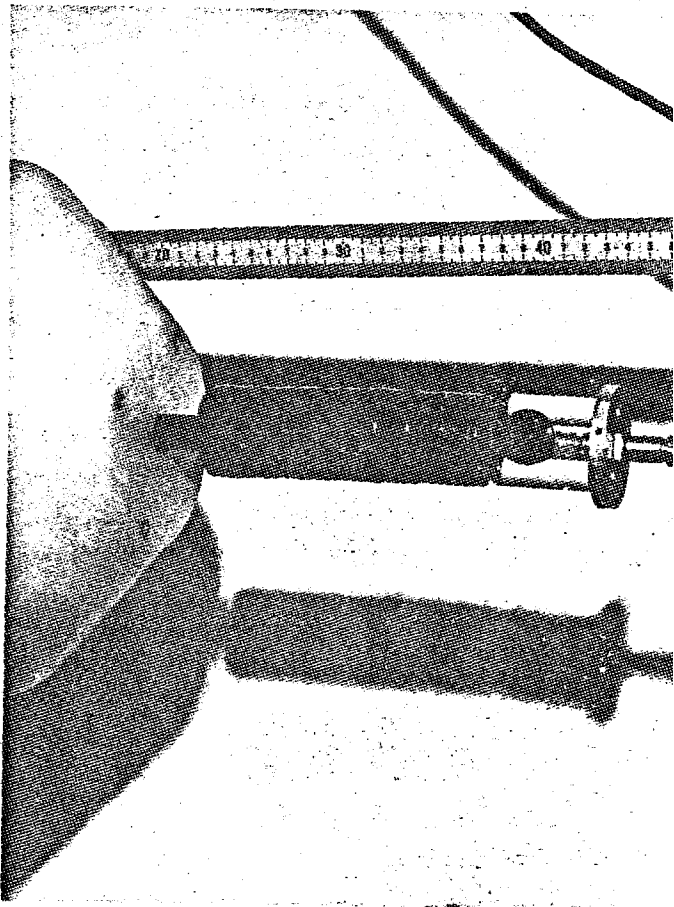


Figure 4

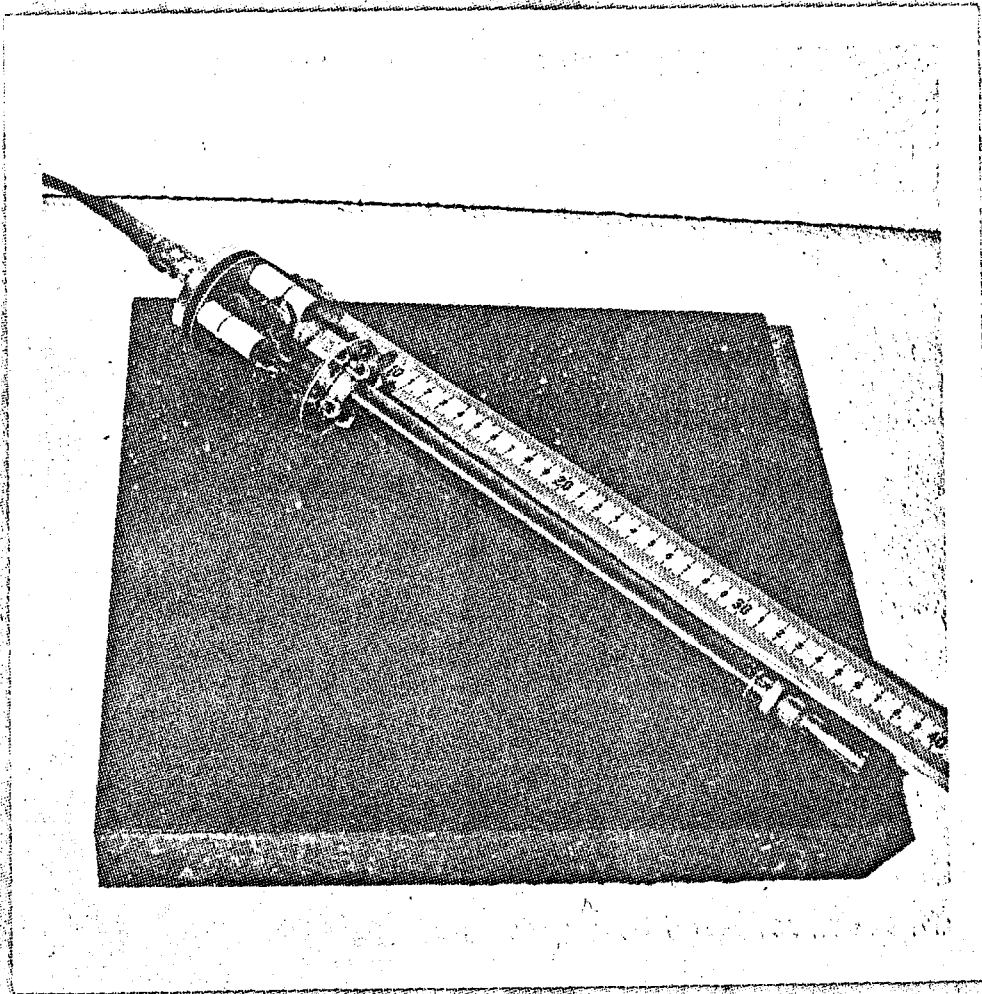


Figure 5

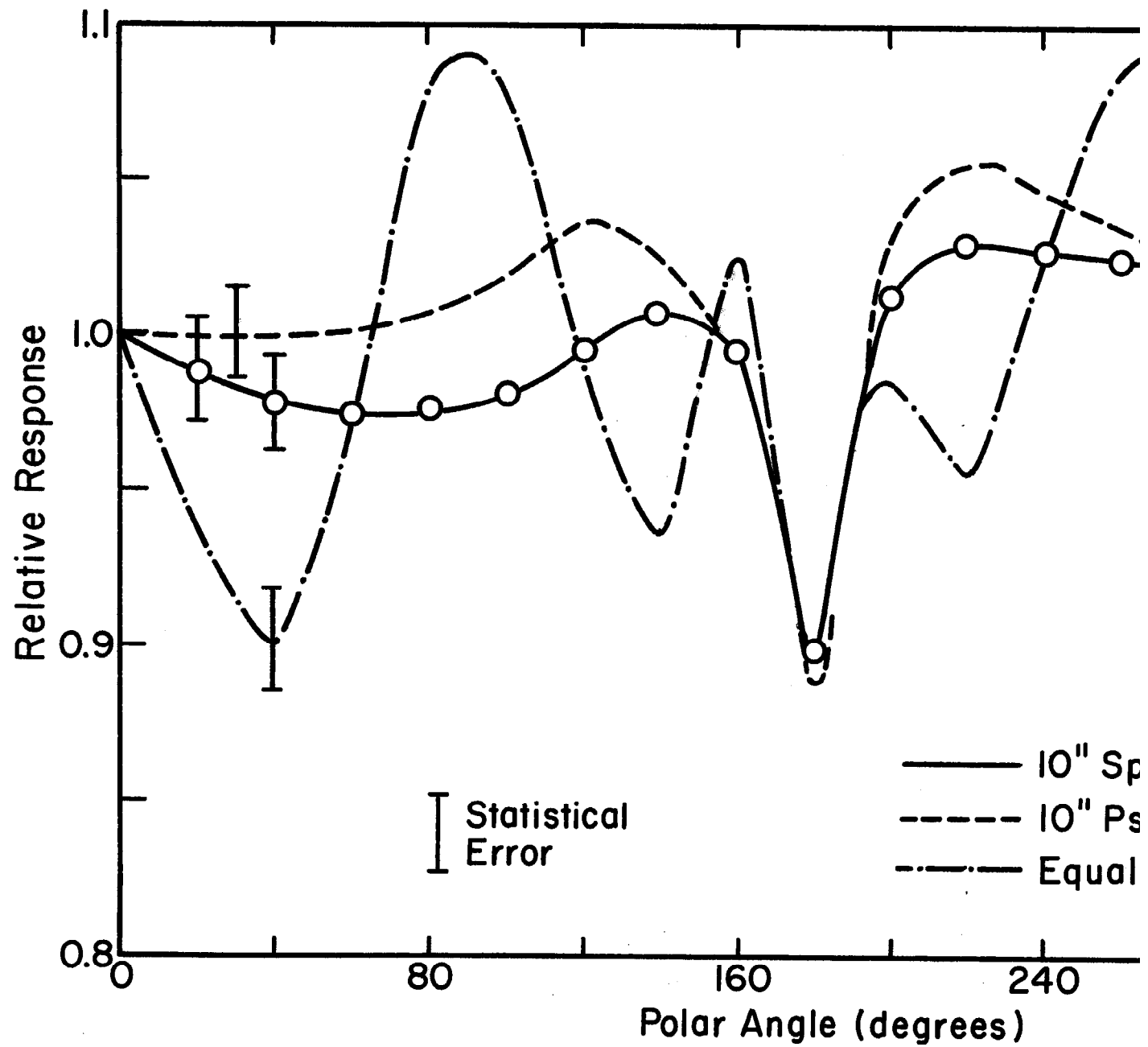


Figure 6

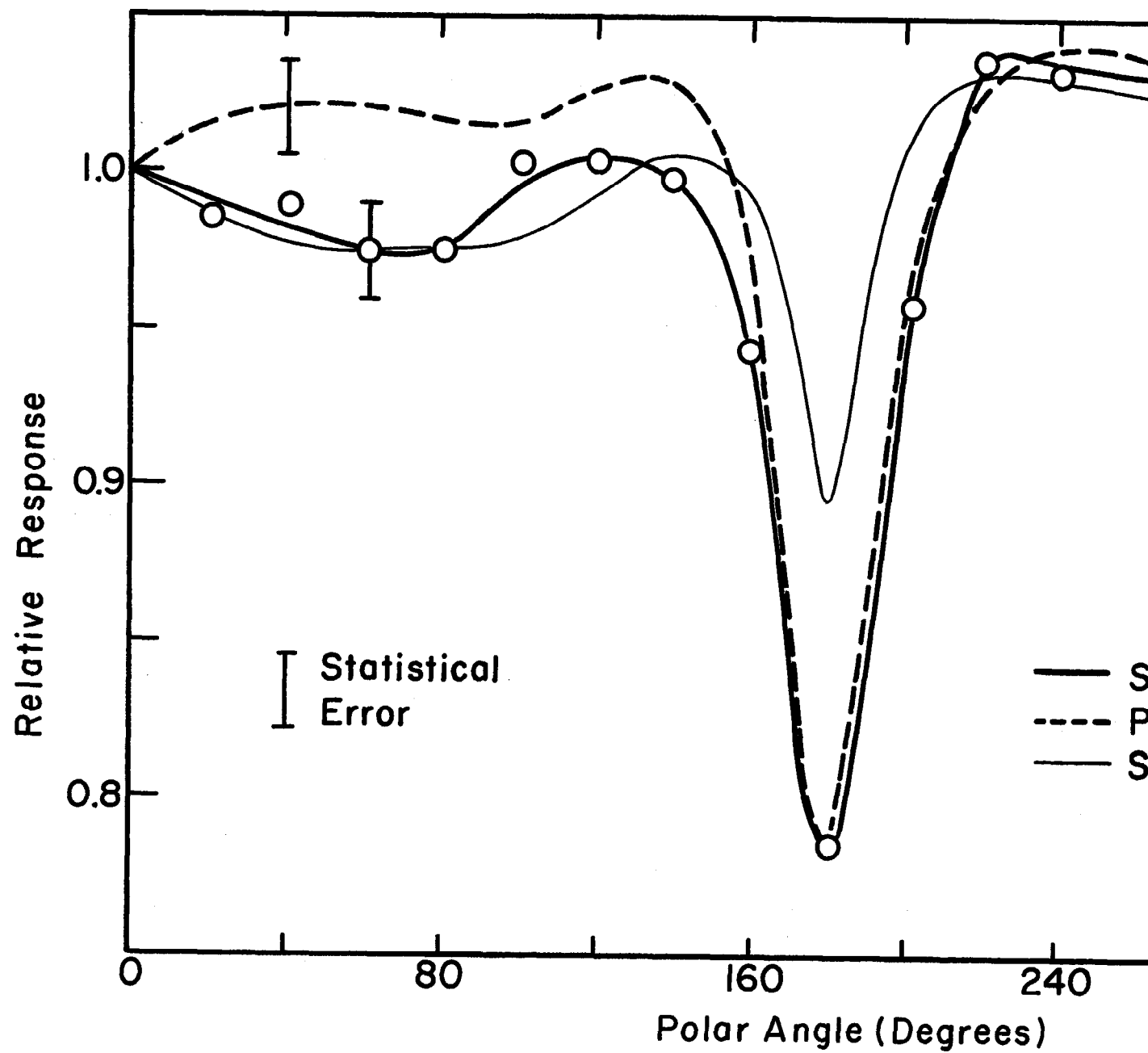


Figure 7

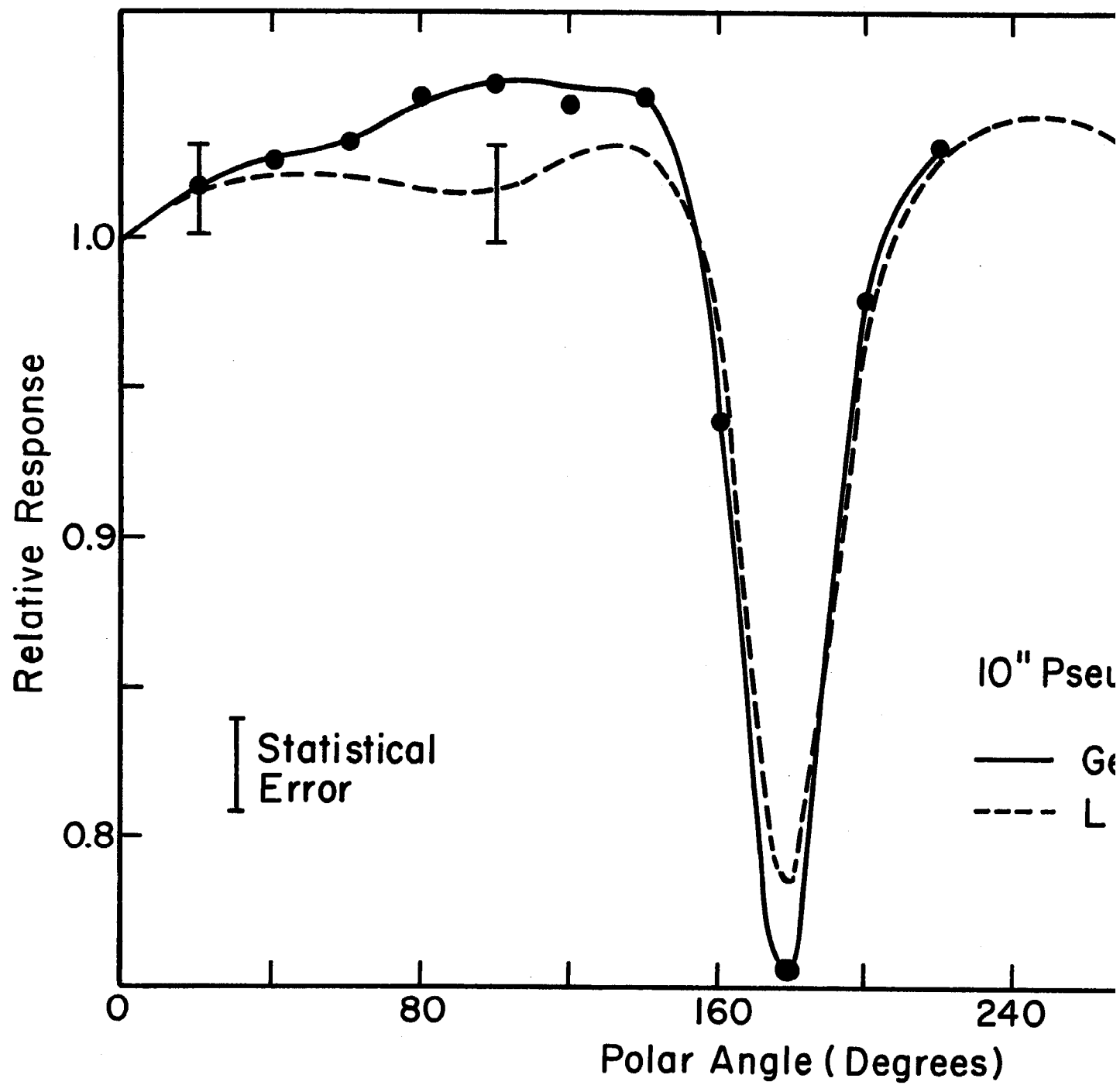


Figure 8

